In situ and interrupted-growth studies of the self-assembly of octadecyltrichlorosilane monolayers

A. G. Richter, C.-J. Yu, A. Datta, J. Kmetko, and P. Dutta

Department of Physics and Astronomy, Northwestern University, Evanston, Illinois 60208-3112

We have examined the self-assembly process of octadecyltrichlorosilane on silicon using x-ray reflectivity. By comparing the commonly used ''interrupted-growth'' characterization technique with results obtained *in situ*, we have determined that quenching the growth and then rinsing and drying the sample introduces free area into the film, presumably by removal of non-cross-linked (physisorbed) molecules. Reintroduction of a quenched and rinsed film to solvent does not restore the thickness of the film to its previous value. We have also performed *in situ* growth studies over a range of concentrations. For all concentrations, we observe growth of islands of vertical molecules. The growth follows Langmuir kinetics, except at short times for low concentration solutions.

PACS number(s): 68.45.−v, 82.65.My, 81.15.Lm

I. INTRODUCTION

Self-assembled monolayers (SAMs) are single layers of organic molecules chemically adsorbed onto solid substrates. There are many classes of molecules that will form SAMs, all of which contain a head group that bonds to the surface, the body of the molecule, and an end group. SAMs are most commonly formed by immersion of a substrate into a dilute solution of these molecules in an organic solvent. The process is self-limiting and the resulting film is a dense organization of molecules that are arranged so that they primarily expose their end groups. SAMs have been widely studied because of this property: by functionalizing the terminal group, very precisely arranged molecular arrays can be created for applications ranging from simple, ultrathin insulators and lubricants to complex biological sensors.

Despite their promise, many fundamental questions still remain concerning the growth of SAMs. Until recently, all of the studies of solution-grown SAMs that examined incomplete films were performed using an interrupted-growth technique [1–14]. Substrates were dipped in solution and then after a certain amount of time, the growth was quenched. The samples were then rinsed and characterized *ex situ*. This method provides some opportunity for morphological changes in the film, as the local environment is radically altered during the growth. Therefore, this technique may not reliably indicate what is actually occurring during deposition. This was the main impetus for our *in situ* studies.

We previously reported the first *in situ* x-ray experiments following the growth of a common SAM material, octadecyltrichlorosilane (OTS), grown on silicon oxide [15]. We determined that the films underwent island growth because the thickness of the film remained constant at that of fully extended molecules, the average density increased monotonically, and the film-solution interface width did not change radically over the duration of deposition. This compares well with atomic force microscopy (AFM) and spectroscopic observations [6–8,10–12,16–18] of OTS on silicon and other, similar systems. However, some x-ray reflectivity, ellipsometry, and infrared experiments indicated that OTS films grow in a uniform manner—the thickness increases with deposition time as the molecules start out highly tilted and stand up

to accommodate newly adsorbing molecules [1–5,19]. Several groups have seen intermediate modes of growth, depending on temperature, water content of the solvent, humidity, etc. [9–11,13,14]. All of the above references used the interrupted-growth technique, except for Woodward and Schwartz [16] and Doudevski *et al.* [17], who studied octadecylphosphonic acid (OPA) on mica with *in situ* AFM; Resch *et al.* [18], who studied OTS on mica with *in situ* AFM; and Vallant *et al.* [19], who studied OTS on silicon with *in situ* IR.

In order to address the inconsistencies between our island growth result and those interrupted-growth studies that display uniform growth, we deposited the same OTS films on silicon that we had studied *in situ*, but instead used the interrupted-growth method. In this way, we hoped to investigate the effect of rinsing on film morphology, the role of the solvent beyond just supplying the adsorbate molecules to the surface, and to eliminate inter-laboratory and substrate preparation differences as a possible reason for the inconsistencies between various studies.

We also performed more *in situ* growth studies while varying the concentration of the solution. In order to perform reflectivity scans, which can take up to 1 h per time step, very low (micromolar) concentrations had to be used to slow down the deposition for the studies reported in [15]. By streamlining the alignment and scanning processes, and by reducing the number of data points and the collection time for each point, we have been able to follow the growth at higher concentrations. We wished to study the growth time scales and mode as a function of concentration to verify that our previous results were not due to our low concentration solutions.

Additionally, we fit each density curve we obtained from the *in situ* studies to a growth model to analyze the kinetics of the reaction. Simple systems should undergo Langmuir growth; this model assumes noninteracting adsorbate molecules, no adsorption after monolayer coverage, a small diffusion rate relative to the desorption rate, and a fixed number of equivalent binding sites. Because OTS forms crosslinkages with neighbors it would seem to violate the noninteraction assumption, but Langmuir-like kinetics also appear in complex systems because the Langmuirian saturated ex

ponential form is a limiting form for many modes of growth. Therefore, we used this functional form as the first step in analyzing the growth kinetics.

We used x-ray reflectivity to characterize these systems. X-ray reflectivity (XRR) and AFM are complementary techniques. XRR samples the whole film within the x-ray footprint (typically on the order of 100 mm^2) at once, giving the in-plane average structure and the out-of-plane structure as a function of distance from the substrate. AFM, on the other hand, gives local information, and is only sensitive to the top of the adsorbed molecules. Additionally, since AFM requires using a finite sized tip, it is insensitive to very small islands, whereas XRR can detect very low film densities. However, XRR is not suited for determining some important growth information, such as the number of islands per site and the island size distribution.

The theory of XRR has been discussed in great detail elsewhere and so only a short discussion will be presented [3,20,21]. XRR samples the structure of a film normal to the surface by keeping the incident and exiting angles equal to each other, the θ-2θ condition. The momentum transfer, restricted to the z direction, is $q=q_z=(4\pi/\lambda)\sin\theta$. Because the index of refraction of all materials at x-ray wavelengths is slightly less than unity, total external reflection occurs for all incident angles up to some critical angle θ_c, which depends on the electron density of the material and the wavelength of the x rays. The critical momentum transfer q_c is independent of wavelength and is equal to 0.0316 Å^{-1} for silicon, corresponding to a critical angle of 0.155° at 11.5 keV. The Fresnel reflectivity for an ideally sharp interface is

$$R_F = \left| \frac{q - \sqrt{q^2 - q_c^2}}{q + \sqrt{q^2 - q_c^2}} \right|^2. \tag{1}$$

For any other interface, there is some density function $\rho(z)$, averaged over the x and y directions. For x rays to reflect there must be a gradient in the electron density; x rays that reflect off of different interfaces in a film interfere with each other, creating a series of maxima and minima in the detected reflectivity. In the Born approximation, we have

$$\frac{R}{R_F} \propto \left| \int \left\langle \frac{d\rho}{dz} \right\rangle e^{iqz} dz \right|^2. \tag{2}$$

Structural information can be obtained from the reflectivity data by assuming a model for electron density profile and then fitting the reflectivity curve by varying model parameters. A typical model is the Gaussian-step model [3]. This model assumes that the film consists of regions of constant electron density, between which the interfaces are error functions (derivatives of which are Gaussian). The reflectivity then becomes

$$\frac{R}{R_F} = \left| \sum_{i=0}^{N} \frac{\rho_i - \rho_{i+1}}{\rho_0} \exp(-iqD_i)\exp\left(\frac{-q^2\sigma_{i+1}^2}{2}\right) \right|^2, \tag{3}$$

where N is the number of layers (the number of interfaces is $N+1$), $D_i = \Sigma_{j=1}^{i} T_j$ is the distance from the silicon surface to the ith interface, T_i is the thickness of the ith layer, ρ_i is the electron density of the ith layer, σ_i is the iterfacial width
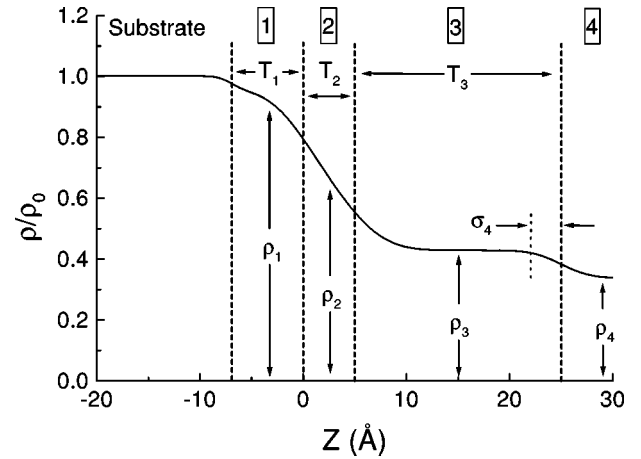

FIG. 1. An electron density profile, demonstrating the definition of the parameters in a typical three-layer Gaussian-step model. For our fitting, region 1 is the silicon-oxide layer, region 2 is an interfacial region, region 3 is the OTS film, and region 4 is either the solvent for *in situ* studies, or helium for *ex situ* studies.

of the ith interface, and ρ_0 is the electron density of the substrate ($=\rho_{Si}$). ρ_{N+1} is taken to be 0 for *ex situ* scans and is the electron density of the solvent for *in situ* scans. Figure 1 shows $\rho(z)$ for a three-layer model.

II. EXPERIMENTAL DETAILS

The silicon (111) pieces were cut from 3 in.×1 in.×0.1 in. samples obtained from Semiconductor Processing, Inc. to measure 5 mm×1 in.×0.1 in. so as to fit into our *in situ* cell. The substrates were prepared using a common cleansing technique. First, they were placed in a piranha solution (a 70:30 vol/vol mixture of sulfuric acid and 30% hydrogen peroxide) and heated to 100°C for 1 h. After cooling for about 10 min, the substrates were rinsed with ultrapure water (10^{18} MΩ cm). Then they were ultrasonicated in an RCA solution—water, H_2O_2, ammonium hydroxide (5:1:1 v/v)—for 30 min. And finally, they were again rinsed with copious amounts of ultrapure water and stored in water in sealed containers until used.

The OTS was obtained from United Chemical Technologies (99%) and used as received. It was stored in a refrigerator and in the dark until used. Heptane (Aldrich; 99%, anhydrous), ethanol (Aldrich; reagent, denatured, anhydrous), methanol (Aldrich; 99.8%, anhydrous), and acetone [Aldrich; 99.9+%, high-performance liquid chromatography (HPLC) grade] were also used as received. The heptane, ethanol, and methanol were left unopened until placed in a glove bag filled with nitrogen. All glassware that was to come into contact with the samples, solutions, or solvents was washed with detergent, rinsed with copious amounts of ultrapure water, sonicated in acetone for 30 min, dried for >8 h in a sealed oven at ~120°C, and then transferred immediately into the glove bag, where nitrogen was passed over it for ~20 min.

The OTS solutions in heptane were made and kept in the glove bag in a presilanized, covered, glass, 100 ml container for a maximum of 4 days. Solutions of varying concentrations were made, ranging from 0.1% (2.5 mM) to 10^{-4}% (2.5 μM) by volume. No visible condensation of the OTS occurred at any concentration while the solution was being
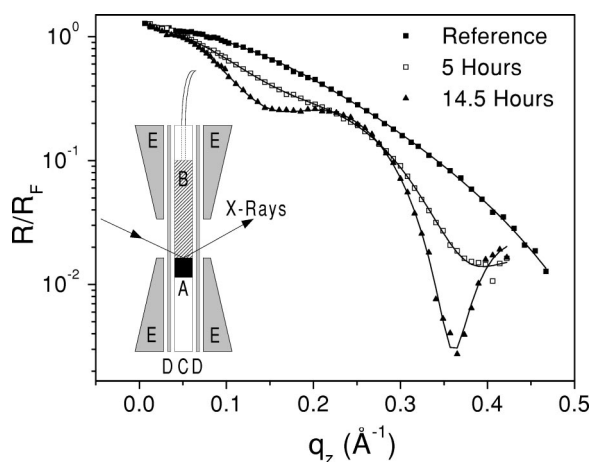
FIG. 2. Three of the *in situ* reflectivity scans taken during film growth of OTS on silicon. The solid lines are fits to the data (see text). The reference scan is obtained prior to deposition under clean heptane. The inset is a schematic diagram of the *in situ* cell: *A*, silicon; *B*, solution chamber; *C*, inner Teflon piece; *D*, beryllium plates; and *E*, stainless-steel frame (taken from [15]).

stored or used. OTS was added to heptane by syringe, agitated by a glass rod for 5 min and left to mix for 15 min. For the lower concentration solutions, higher concentration solutions would be diluted in steps by taking 1 or 10 ml of solution and putting it into 99 or 90 ml of clean heptane, until the desired concentration was achieved. While care was taken to ensure control over concentration levels, reported concentrations should be only taken to be accurate to within $\pm 30\%$. The samples were at room temperature (not separately temperature controlled).

The *in situ* cell is based on a design by Nagy *et al.* [22]. It consists of a Teflon piece 5 mm thick that has a cut-out section that holds the silicon substrate in place and provides a cavity for about 6 ml of solution. The Teflon piece is sandwiched between two 0.01-in.-thick beryllium plates. This assembly is further sandwiched between two stainless-steel pieces that provide structural support. Windows in the stainless-steel pieces allow x rays to pass through. Solution is drawn into and removed from the chamber via Teflon inlet and outlet tubes in the inner Teflon piece. The inset of Fig. 2 is a schematic of the *in situ* cell as viewed from the side. Also shown in Fig. 2 are several of the *in situ* reflectivity curves taken during film formation.

Assembly of the cell and introduction of the solution were performed in the glove bag. For *in situ* studies, the substrate was first examined under clean heptane to obtain reference scans. Then, the solution was introduced at time zero and the cell was mounted on the diffractometer. No further agitation of the solution was performed. Samples were also made outside the *in situ* cell by placing substrates into solution in a glass container in the glove bag, agitating with Teflon tweezers for ~5 min, and then letting them sit. After film formation, the samples were removed, either from the solution container or from the *in situ* sample holder. The samples were rinsed several times with clean heptane, then rinsed repeatedly with methanol, and finally multiple times with ethanol. Samples were removed from the glove bag while in ethanol, then blown dry with nitrogen. If there was evidence of unreacted or unattached OTS on the surface, i.e., a white

powder on the surface or very thick films as evidenced from reflectivity, or if the sample was left in air or ethanol for extended (>1 h) times, the sample was sonicated in acetone for 10 min and then rinsed with ethanol and blown dry with nitrogen. All samples were hydrophobic after removal from solution as evidenced by large water contact angles. When performing *ex situ* scans, the same chamber was used. In this case, the chamber was purged with helium and a slight over-pressure was maintained in order to minimize x-ray background scatter from the air and to lessen x-ray damage.

X-ray reflectivity was performed on beam lines X6B and X23B at Brookhaven National Laboratories' National Synchrotron Light Source (NSLS), and at Sector 10 Materials Research Collaborative Team (MRCAT) at Argonne National Laboratories' Advanced Photon Source, at energies of 11.5 keV ($\lambda = 1.078$ Å) and 11 keV ($\lambda = 1.127$ Å). The incident slit size was set to be 0.15 mm vertically by 2.8 mm horizontally. The scatter slits and detector slits were set to be larger, 0.3 mm by 3 mm.

III. RESULTS

A. Fitting

Each *in situ* reflectivity curve was fit using a three-layer Gaussian-step model: a silicon-oxide layer, an interfacial layer, and the OTS film layer. The silicon dioxide parameters are generally held constant, except for the thickness, which is determined for each substrate and then held constant for each reflectivity scan on that substrate. The electron density of silicon oxide is $0.96\rho_{Si}$ [3]. Typical thicknesses are 5–15 Å. Since x rays are sensitive to electron density gradients, if there is only a small density difference between layers in the film, the x rays will only weakly scatter from it, making it difficult to detect. This also means that the reflectivity curve, and hence our fits to it, are quite insensitive to small changes in the interfacial width between silicon and silicon oxide, so we hold it fixed at 1 Å or 2 Å.

The interfacial layer is between the oxide and the film. It is common practice to add this interfacial layer to take into account the head-group region of the film [3]. Quite often in the literature, this layer has an electron density greater than that of silicon. In our case, the density of this layer is always between that of the film and the silicon. The thickness of this layer also varies over deposition time, though that variation is not monotonic. However, a range of interfacial layer and film layer thicknesses give comparably good fits if their sum is unchanged. Therefore, we identify the interfacial layer thickness as part of the total OTS film thickness. This is further motivated by the fact that this interfacial layer is not discernable as a distinct layer in the electron density profile, but rather serves mainly to broaden the interface between the oxide and the film. It is unfortunate that our *in situ* reflectivity scans are limited by the solvent-scatter background to ~0.5 Å^{-1} in q_z, as this limits our ability to ascertain the physical nature of this thin interfacial layer. It seems quite possible that it is indicative of the hypothesized water layer [9,23–27]. Or it could be evidence of retention of chlorine atoms, either from unhydroxylated chlorosilane groups, or by retention of solvent in the film, though several studies have shown that no solvent or chlorine is present after film formation [2,28–30]. It could also be water that is hydrogen

TABLE I. Comparison of the parameters from a fit of the final *in situ* scans with the parameters from the reflectivity scans measured after rinsing and removing the samples and scanning under helium (*ex situ*).

Sample name	Concentration (mM)	Final *in situ*		*ex situ*		% change	
		ρ/ρ_{Si}	T (Å)	ρ/ρ_{Si}	T (Å)	ρ/ρ_{Si}	T
$S1$	0.0025	0.429	25.74	0.398	23.79	−7.23	−7.58
$S2$	0.0025	0.428	24.13	0.386	23.23	−9.81	−3.73
$S3$	0.0025	0.449	26.76	0.398	24.49	−11.36	−8.48
$S4$	0.025	0.432	25.34	0.401	24.60	−7.18	−2.92
$S5$	0.25	0.428	23.87	0.371	23.34	−13.32	−2.22
$S6$	2.5	0.426	23.96	0.413	23.75	−3.05	−0.88
$S7$	2.5	0.438	24.44	0.413	24.25	−5.71	−1.27

bonded to unpolymerized silanol groups [4,28,31,32].

It has been found that a fully formed OTS monolayer has a thickness of about 25 Å and a density of $0.43 \pm 0.05 \rho_{Si}$ [1–3]. Each carbon-carbon (C-C) bond is 1.55 Å in length and C-C-C bond angle is 110°, giving an extension in the z direction per CH_2 of 1.26 Å . There are 17 C-C bonds, plus 1.92 Å for the third H atom in the terminal methyl group, plus the C-Si bond of 1.52 Å , giving a total of 24.86 Å . This ignores the Si-O bond associated with the molecule which is assumed to contribute not to the XRR measured film thickness, but rather to the oxide thickness [1]. Since we include the interfacial region in the film thickness, it is appropriate to add 1.34 Å for the Si-O bond, bringing the total film thickness to 26.2 Å . The typical surface roughness of an OTS SAM on polished silicon or mica is 2–4 Å.

We used heptane as the solvent. Heptane has an electron density of $0.34 \rho_{Si}$, which we hold constant in the fitting process. Since we are using a ''transmission *in situ* cell'' rather than a ''reflection *in situ* cell,'' the solvent layer is macroscopically thick and taken to be semi-infinite. Heptane has one of the lowest electron densities of commonly available solvents, and creates a density difference between the solution and the OTS film. However, this difference is still small, and so the reflectivity is not sensitive to small changes in the OTS-solution interface width. We therefore commonly hold this parameter at a reasonable value of 2.0–2.2 Å . It should be noted, however, that changes of 2 Å or greater in this parameter do affect the reflectivity curve, so we are sensitive to large-scale changes in the surface-solution interface should they occur.

The fitting procedure is as follows. First, the reference scan (clean heptane only) is fit to determine the silicon-oxide thickness and predeposited surface roughness. Then the last *in situ* scan is fit, usually allowing all parameters to vary except for ρ_{SiO_2} and σ_{Si-SiO_2}. Usually T_{SiO_2} does not vary much from that of the reference scan, but we find that we cannot usually satisfactorily fit the curves unless we allow it to vary. We then work backwards in time, starting with the final *in situ* scan, fitting each curve using the previous scan's fitted parameters as the starting parameters. In some cases, in addition to the solution-film interface, some of the other interfacial widths become poorly defined because the electron density contrast between adjacent layers is low. In these cases, the appropriate interfacial width parameter is held constant at a typical value (1–2 Å).

Ex situ reflectivity curves are fit with a two- or three-layer Gaussian-step model. Occasionally, we find that for satisfactory fits a layer is required between the oxide and the film, as for the *in situ* samples. This layer is similar to that used by Tidswell *et al.* in that the density is sometimes greater than that of silicon, it is 1–2 Å thick, and it has broad interfaces [3].

B. *Ex situ* comparison

A direct comparison between the structure of a film while in solution and when removed from solution was made in three ways. The first method, also the simplest, was to compare the final *in situ* reflectivity curve with one taken after the same sample was removed from the cell and rinsed and then placed under helium. For the second method, a sample's growth was followed *in situ* and then the sample was rinsed and reimmersed in heptane and rescanned. And the third method was the preparation of a series of interrupted-growth samples by removing substrates from solution before complete monolayer formation could occur and then scanning under helium.

The first method was performed numerous times with many different *in situ* examined samples. *In situ* scans were usually taken until no change could be seen in the reflectivity curve, after which it was assumed that the growth was finished. Then the sample was removed and rinsed, using the method described above. In all cases, the fits to the reflectivity curve showed that the thickness and the density were lower after rinsing than during the last *in situ* scan. Table I shows the film thickness and density for the final *in situ* scans and for the *ex situ* scans. Figure 3 shows the electron density profiles of the final *in situ* scan and the *ex situ* scan for sample $S1$. The decrease in density and thickness is clearly visible.

The second method was performed to determine what would happen after placing a quenched and rinsed sample back under solvent. After following the growth of sample $S7$ *in situ* until it appeared to be finished, the standard rinsing procedure was used. Then, the sample was put back under heptane and examined. Additionally, a sample $S8$ that was prepared with the same solution and for the same amount of time but that had not been previously exposed to x rays was treated in the same manner. Figure 4 shows the electron density profiles obtained by fitting the reflectivity curves (shown in the inset). It is clear that after rinsing, the thickness and
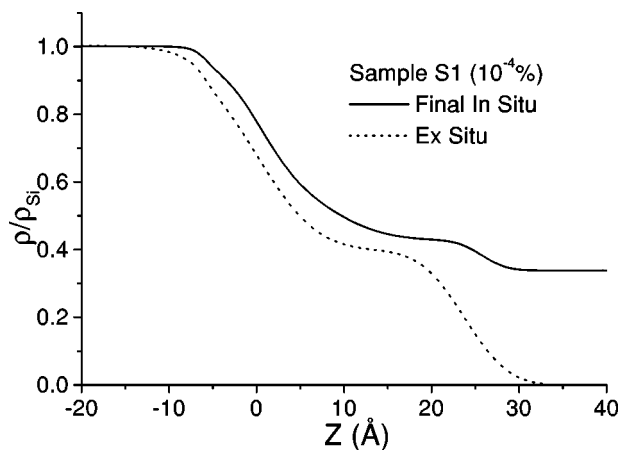
FIG. 3. The electron density profiles from a final *in situ* scan and an *ex situ* scan from the same sample after rinsing.

density of the film decrease somewhat and that placing under heptane does not return the thickness to its previous value. A fit to the reflectivity curve of $S7$ taken under heptane gives an electron density of $0.410\rho_{Si}$ and a thickness of 23.64 Å compared to $0.438\rho_{Si}$ and 24.44 Å for the final *in situ* scan. It is also clear that since both the *in situ* cell formed sample and the sample that was grown without x-ray exposure show very similar curves, this is not an effect of x-ray damage.

For the third method, the interrupted-growth study, samples were made and examined directly after growing and studying a sample *in situ* so that the chemistry and substrate conditions would be similar for both sets of samples. The *in situ* sample followed the same trends as the previous *in situ* samples, indicating island growth. Four clean substrates were placed into an OTS solution (2×10^{-3}% by volume, 50 μM) and then removed, allowing several hours between each sample removal to lapse. The samples were rinsed in the standard way and then scanned under a helium environment. The inset of Fig. 5 shows the four reflectivity curves obtained. The minimum in the reflectivity shifts to progres-
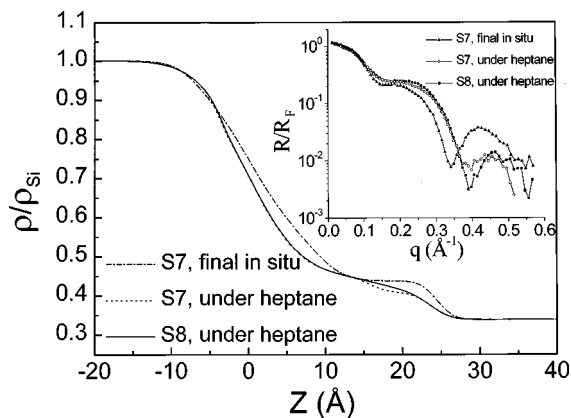

FIG. 4. The electron density profile for a sample ($S7$) that was studied while *in situ*, then rinsed and put back under solvent. The third profile is from an additional sample ($S8$) that was prepared and scanned in the same manner, but which was not previously exposed to x rays. The inset shows the corresponding reflectivity curves. After rinsing, the minimum position shifts to a higher q, indicating a decrease in thickness. Reimmersion in solvent does not restore the film to its full thickness.
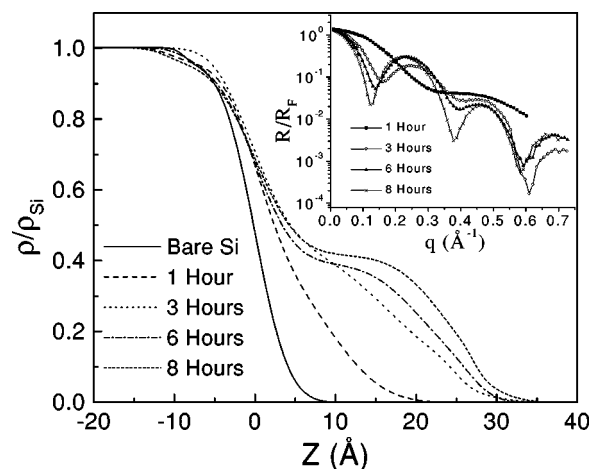

FIG. 5. An interrupted-growth study. Each reflectivity curve (shown in the inset) was obtained from a sample that was removed from solution prior to full film formation. The progression of the minimum position to lower q values with deposition time indicates that the film thickness increases, implying a uniform mode of growth. The corresponding electron density profiles are shown in the main panel. At early times, the film thickness is low. At intermediate times, the thickness increases, but the film density is highly nonuniform across the film's extent, indicating that the molecules have a range of tilts. At later times, the film becomes more uniform and approaches the thickness of fully extended OTS molecules.

sively lower and lower q values, indicating that the film gets thicker over deposition time, consistent with earlier reports [1–5,19]. The main panel of Fig. 5 shows the electron density profile obtained from fitting the reflectivity curves. At early times, the film is less extended and is lower in density. At medium times, the electron density appears to be broadened across the extent of the film, suggesting that the molecules have a range of tilts. Finally, at larger times, the film becomes more uniformly dense and approaches its fully formed thickness and density.

C. Concentration dependence and growth curves

In situ studies were performed at various concentrations, ranging from 10^{-1}% to 10^{-4}% by volume (2.5 mM to 2.5 μM). All of the reflectivity scans showed similar behavior as to the 10^{-4}% sample reported previously [15]. However, the high concentration samples ($>10^{-2}$%) grew so quickly that good fits to the curves could not be obtained until late in the growth when changes in the film morphology slowed. Figure 6 shows the electron density of the film layer as a function of deposition time for all of the samples whose curves we could fit. In each case, the electron density increases over deposition time, while the thickness (not shown) stays constant, just as with the published 10^{-4}% data.

Each of the density vs time curves is the growth (coverage vs time) curve, since the film thickness is constant during *in situ* growth. One of the simplest and most common growth modes is Langmuir in which the rate of coverage increase is proportional to the uncovered space on the surface

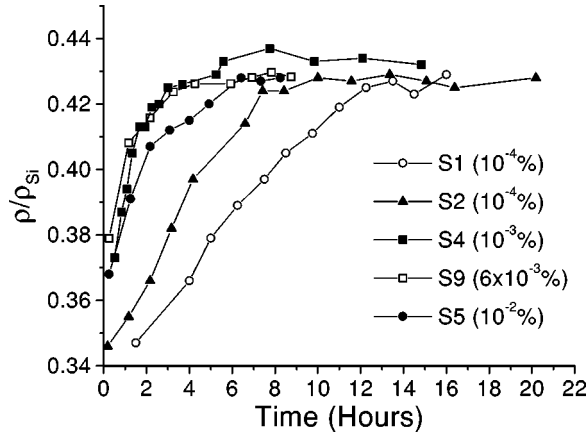$$\frac{d\theta}{dt} = F(1-\theta), \qquad (4)$$

FIG. 6. Density curves for different solution concentrations. Each curve has approximately the same shape, and for all concentrations constant thickness growth is observed.

which leads to

$$\theta = 1 - e^{-t/\tau}, \tag{5}$$

where F is the adsorption rate, and τ is the growth time scale ($=1/F$). In this model, the adsorbed molecules are assumed to be noninteracting, merely serving to block molecules in solution from landing on the surface.

We attempted to fit Langmuir curves to our growth curves. We converted the density to coverage using the equation

$$\theta = \frac{\rho_{\text{film}} - \rho_{\text{solution}}}{\rho_{\text{complete}}}, \tag{6}$$

where ρ_{solution} is $0.34\rho_{\text{Si}}$ and ρ_{complete} is found by fitting the density data to a modified Langmuir function. Note that we have already determined that the films grow by formation of vertical islands, and we have found no evidence for either interposed tilted molecules or separated regions of tilted molecules. The parameter ρ_{film} is the density of the film near the film-solution interface and would include both physisorbed and chemisorbed molecules, but only those that are vertical or nearly so. Therefore, the coverage we calculate is the coverage of islands, which can include both chemisorbed and physisorbed molecules. The curves from the lowest concentrations show a deviation from a Langmuir shape at early times. We cannot adequately fit these curves unless we exclude these points from the fit and allow for a time offset before Langmuir kinetics begin. If we do so, we get quite good fits to the rest of the data using the form

$$\theta = 1 - e^{-(t-t_0)/\tau}, \tag{7}$$

where t_0 is the time offset. Figure 7 shows several of these fits and Table II shows the parameters.

The growth curves obtained for the highest concentration samples are of obvious poorer quality than the lower concentration samples because the quicker growth limits the number of scans we can take and because the film changes during the reflectivity scan. The errors in the data points, and hence the time offsets and growth timescales, are only approxi-
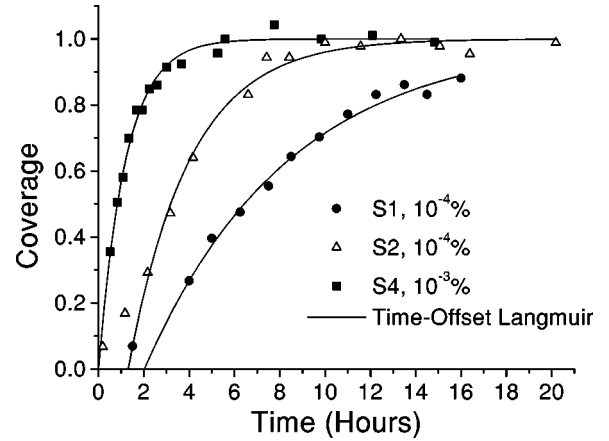

FIG. 7. Fits to the density curves for three of the samples ($S1$, $S2$, and $S4$). The curves follow Langmuir kinetics, although there is a deviation at early times for the low concentration solutions that requires the inclusion of a time offset.

mate, calculated by averaging the errors obtained by rigorous analysis of our previously published data on sample $S1$. The actual errors for the higher concentration samples would be expected to be larger, and the time axis is imprecise as well.

IV. DISCUSSION

A. *Ex situ* comparison

The first two comparison methods show that quenching the growth before full film formation causes the thickness and the density to decrease. Rinsing also appears to cause an irreversible process to occur, as reimmersion in solvent does not restore the film to its prerinsed thickness. Combining these two findings leads us to propose that the solvent molecules help keep the adsorbed molecules vertical and that rinsing the film causes some of the non-cross-linked molecules to be removed from the film, creating free volume. Some of the molecules then tilt over, lowering the thickness. The fact that the density, on average, decreases more than the thickness indicates that there are regions of relatively dense regions of molecules that do not tilt much or at all and regions that lose most of their molecules after rinsing. This could be explained by most of the loss of molecules coming from the perimeter of the islands, allowing molecules on the perimeter to tilt somewhat, but keeping those in the interior relatively vertical.

Several studies have proposed that the OTS molecules do not fully cross-link until late in the deposition process and that the degree of polymerization depends on water content

TABLE II. Parameters from fits of the growth curves to a time-offset Langmuir model.

Sample	Concentration (mM)	t_0 (h)	τ (h)
$S1$	0.0025	2.02 ± 0.15	6.35 ± 0.22
$S2$	0.0025	1.31 ± 0.13	2.70 ± 0.18
$S4$	0.025	0	1.19 ± 0.03
$S9$	0.15	0	0.54 ± 0.08
$S5$	0.25	0	1.40 ± 0.16

of the solution [4,13,32,33]. Furthermore, there appears to be only minimal direct attachment of OTS molecules to the surface [4,9,25,28,31,34], meaning that the molecules must attach to one another to form a complete film. XRR is sensitive to the presence of both the chemisorbed and physisorbed molecules and does not differentiate between the two if both species have the same orientation. The act of rinsing an incomplete film may then remove the physisorbed molecules that are only held in place by hydrogen bonding to neighbors and possibly to the proposed water layer on the oxide. After the molecules tilt to fill in the free volume, reimmersion into solvent does not appear to untilt them. After rinsing and drying the film, the heptane molecules do not interpose themselves into the film, as they presumably do during growth [35].

Resch *et al.* performed a series of ''stopped flow/deposition'' experiments of OTS on mica in which after a period of exposure to solution, pure solvent was flowed over the sample to halt deposition and allow AFM characterization [18]. They found that the islands were always the same thickness of 25 Å , regardless of size. That the molecules do not appear to tilt after rinsing is in opposition to what we see in our experiments, but it could be that since their film was never removed from solvent and dried, there was no opportunity for molecules to fall over, as they may be impeded by the presence of solvent molecules. The stopped flow/deposition images also appear to be very similar to their ''continuous flow'' images (AFM scans done while deposition occurred), which further implies that either all the molecules they observe are cross-linked, or rinsing without drying does not fully remove physisorbed molecules. A rough comparison with their *in situ* and *ex situ* examined samples shows that samples that are removed from solution and dried display a larger variation in island size and shape than those scanned while still in solution or solvent.

The interrupted-growth study confirms our suspicions of the inconsistencies between our *in situ* results and the results of other groups' studies that report uniform growth. Our *in situ* observation of island growth was not due to various unquantified differences between different groups in experimental conditions and procedures, but rather it is the act of quenching and rinsing that causes this discrepancy; the actual mode of growth while in solution is through the formation of uniformly thick islands. Substrate and solution water level differences, and perhaps temperature and clean room conditions, can certainly alter the film morphology and this may be partially responsible for some of the different growth mode observations. Our study shows, however, that even with the same growth conditions that give rise to island growth and the formation of well-packed complete monolayers, removal from solution, rinsing, and drying does cause a change in the characteristics of the film that can be interpreted as being uniform growth.

Figure 5 distinctly shows that at intermediate deposition times, molecules have a range of tilts, further supporting the hypothesis that rinsing removes some randomly arranged physisorbed molecules and allows the remaining molecules to tilt. Our *in situ* studies confirm that the growth occurs through the formation of vertical islands, so any tilt of the molecules must arise after rinsing. Because the islands have the density of a fully formed film while in solution, the mol-

ecules must either tilt to fill in vacancies left by molecules that have been removed form the film, tilt away from the islands along the island edges, or a combination of both. Vallant *et al.* [14] also detected a range of tilts for incomplete OTS monolayers on silicon deposited using the interrupted deposition method, attributing most of this disorder to small islands that have a random distribution of heights as compared to larger islands that have a uniform height. They suggest that at early times, most of the film is disordered and the formation of ordered regions (islands) occurs slowly at first and then rapidly towards the end of deposition. However, because our *in situ* studies show that the islands have a constant thickness and the film increases in density over deposition time, we can be certain that their observation of disorder at early times is due to quenching and rinsing, unless this disorder exists for a short enough time that it disappears before we can perform an *in situ* scan.

B. Concentration studies and growth curves

Our previously reported growth data was obtained for very low concentration solutions (10^{-4}%, 2.5 μM, by volume). Since most of the published work on the OTS-Si system was done with millimolar concentrations, there was some concern that there could be a difference in growth mode between these widely different concentrations. In addition, when we first attempted to fit the density curve to a Langmuir function, we found that if we were to accept the first point as part of the curve, we could not achieve a good fit. It appeared, in fact, that the density curve followed a more linear function until reaching the fully formed film density, which would be indicative of a lack of solute molecules reaching the surface. A rough calculation of the number of molecules in the solution showed that there were only approximately 30 times the number of molecules needed to fully cover all sides of the silicon substrate with a monolayer. These realizations led us to question whether or not our results were influenced by the minute concentration of the solution and hence were not representative of the growth done at more elevated concentrations. For this reason we made several *in situ* studies at various concentrations, ranging from 10^{-1}% to 10^{-4}% by volume. A systematic study of growth time scales at different concentrations could also, in theory, illuminate some aspects of the kinetics of the growth of these SAMs—do the molecules preassemble in the solution as proposed by some, or is the film built up by monomer interactions on the surface?

Each set of *in situ* data was fit as described above. In all cases, the thickness remained approximately constant while the density increased. Several of the data sets show slight differences in the properties of the interfacial layer, but this may not imply a real difference in the environment near the surface, but may rather be indicative of the shortcoming of the model to adequately describe the electron density profile of a broadened interface. The main difficulty in studying the growth at higher concentrations is that the growth occurs so rapidly that each scan is not a ''snapshot'' and only a few scans can be obtained before the growth is complete. Therefore, the higher concentration data is not as well defined as the lower and the fitting is consequently looser. We found that we could not fit the data for the 10^{-1}% concentration at

all, except at late times, presumably because the films changed too much during the early scans. Comparison of each of the density curves we obtained after fitting those that we could shows that each follows the same general trends. The lowest concentration sample is not anomalous; rather, at all solution concentrations studied, the molecules are vertical during deposition. In addition, we saw no evidence for the onset of multilayer growth that several groups have seen in *ex situ* samples [36–38].

As to be expected, as the concentration increases, there is a general decrease in the growth time scales (an increase in the growth rate) (see Fig. 6). However, we do not observe a monotonic decrease. This is most likely due to the fact that we do not have adequate control over all the important chemistry parameters, such as substrate conditions, solution water levels, humidity, and temperature. It is well documented that a variation in any of these parameters leads to a variation in the speed of film formation and in some cases, the quality of the film [2,4,10–12,14,23–25,28,36].

Except for deviations at short times, the growth does appear to follow Langmuir kinetics. However, as stated above, Langmuir kinetics can be observed for more complicated interactions in limiting cases. The adsorption rates $(1/\tau)$ that we find range from 4.4×10^{-5} s^{-1} for the slowest growing sample $(2.5 \ \mu M)$ to 4.5×10^{-4} s^{-1} for the fastest $(0.15 \ mM)$. This compares favorably with the value found by Doudevski *et al.* [17] for OPA on mica of $8.1 (\pm 0.5) \times 10^{-5}$ s^{-1} for a solution concentration of 0.1 mM. Our result may imply that OTS does not preassemble before deposition, since OPA cannot and the time scales are similar, unless entire assemblages of molecules have similar kinetics to monomers. This similarity in adsorption rates is also interesting because several studies have found that OTS on mica should grow faster than on silicon under similar conditions [14,39]. Since rinsing removes some OTS molecules, an *ex situ*, interrupted-growth study is likely to observe an artificially slow growth rate. If the effect of rinsing is different between OPA-mica, OTS-mica, and OTS-silicon, this could be interpreted as a difference in time scales for the various systems. In fact, the *ex situ* study of OTS on mica of Valant *et al.* [Ref. [14], Fig. 3(b)] suggests that rinsing might create larger islands and increase the island height, which is different than what we see for OTS on silicon.

Because of our limited time resolution, we cannot discern why there is a deviation from Langmuir kinetics at early times at low concentrations. We have at best two data points in this region, and the size of the error bars rules out any unambiguous complicated, functional fit. There seems to be an inverse relationship between the required time offset and the growth rate, implying that the offset is due to a process that requires a certain number of molecules before switching to Langmuir kinetics. This could be the initial nucleation of the film, which would presumably be slower with a lower impingement rate (concentration).

In their study of a different SAM system, akylthiols on gold, Eberhardt *et al.* [40] also observe Langmuir growth after an initial delay. In their case, this offset is due to an initial phase of lying-down molecules that does not contribute to the signal used to calculate the coverage of molecules in the fully formed film phase. While we are insensitive to molecules that are lying down because of resolution con-

straints, we do observe that even at these early times some proportion of molecules are vertical, so it is unlikely that our system undergoes a similar phase transition as for the thiol-Au system.

The study of OPA on mica of Doudevski *et al.* [17] showed that the growth did not follow a simple, single Langmuir curve. They observed the growth up to a coverage of about 0.3 at 8000 s. At very early times, up to a coverage of 0.1 at 1000 s, they found that the growth appears to be Langmuirian. From 1000 to 4000 s, the coverage did not change appreciably. This was followed by another region of Langmuir growth that presumably continued until full coverage. Interestingly, the time constant for both Langmuir regions is the same, indicating that the kinetics are the same for both growth regions. They suggest that the intermediate region is due to molecular dissolution from island edges, but they argue that this would not happen with OTS molecules because of the cross-linking. However, as discussed above, the cross-linking may not occur until late in the growth, and so this dissolution process may occur for OTS as well, though it would make an explanation of the observed fractal shape of OTS islands on mica and silicon more difficult [7,10,13]. This picture would satisfactorily explain our observed growth curve, as not only do we observe a deviation from Langmuir growth at early times for some samples, but also we see that the coverage is ''too high'' at very early times. That is, the coverage appears to jump to about 0.1 as quickly as we can measure, but then does not change much until Langmuir kinetics begin. Also, sample $S2$, which has a similar adsorption rate to the sample of Doudevski *et al.*, has a time offset of 1.3 h $(4720 \pm 470$ s$)$, which compares well with the onset of the second region of Langmuirian growth for the sample of Doudevski *et al.*, around 4000 s.

Vallant *et al.* in a very recent paper [19] reported using *in situ* attenuated total reflection (ATR) infrared spectroscopy to study the growth on OTS on silicon and have also found that the coverage follows the Langmuir adsorption model. The adsorption rate that they measure for a 1 mM solution (with a water concentration of 2.2 mM) is 2.8×10^{-4} s^{-1}, again very similar to the value we obtained (see Table II). However, this group's study is indicative of the varied types of growth that are seen, depending on the experimental conditions and the characterization method. In a paper by the same group, Resch *et al.* used *in situ* AFM to observe the growth of OTS on mica, finding that growth proceeds by island formation and aggregation [18]. At all times, the film thickness was found to be about 25 Å and the bare mica surface could be seen in regions where there were no islands. However, their *in situ* ATR experiment indicates that during growth, the molecules begin with an average tilt of about 35° and end with an average tilt of 7° as measured from the surface normal. This result indicates uniform growth, though it could also be that the islands tilt as a whole or that there are islands of fully extended molecules surrounded by tilted molecules so that the average tilt is greater than that of a densely packed film. These possibilities all directly contradict their previous *in situ* results, as well as our own, though they agree well with *ex situ* experiments. In any case, the observation of Langmuir growth and the similarities of measured adsorption rates as determined by *in situ* XRR and those found by Vallant *et al.* and Doudevski *et al.* for similar

systems using different characterization techniques strongly suggest that the Langmuir growth model is correct.

ACKNOWLEDGMENTS

[1] S. R. Wasserman, G. M. Whitesides, I. M. Tidswell, B. M. Ocko, P. S. Pershan, and J. D. Axe, J. Am. Chem. Soc. **111**, 5852 (1989).

[2] S. R. Wasserman, Y.-T. Tao, and G. M. Whitesides, Langmuir **5**, 1074 (1989).

[3] I. M. Tidswell, B. M. Ocko, and P. S. Pershan, Phys. Rev. B **41**, 1111 (1990).

[4] D. L. Angst and G. W. Simmons, Langmuir **7**, 2236 (1991).

[5] I. M. Tidswell, T. A. Rabedeau, P. S. Pershan, and S. D. Kosowsky, J. Chem. Phys. **95**, 2854 (1991).

[6] A. Barrat, P. Silberzan, L. Bourdieu, and D. Chatenay, Europhys. Lett. **20**, 633 (1992).

[7] D. K. Schwartz, S. Steinberg, J. Israelachvili, and J. A. N. Zasadzinski, Phys. Rev. Lett. **69**, 3354 (1992).

[8] Y. I. Rabinovich and R.-H. Yoon, Langmuir **10**, 1903 (1994).

[9] D. L. Allara, A. N. Parikh, and F. Rondelez, Langmuir **11**, 2357 (1995).

[10] K. Bierbaum, M. Grunze, A. A. Baski, L. F. Chi, W. Schrepp, and H. Fuchs, Langmuir **11**, 2143 (1995).

[11] A. N. Parikh, B. Liedberg, S. V. Atre, M. Ho, and D. L. Allara, J. Phys. Chem. **99**, 9996 (1995).

[12] D. W. Britt and V. Hlady, J. Colloid Interface Sci. **178**, 775 (1996).

[13] C. Carraro, O. W. Yauw, M. M. Sung, and R. Maboudian, J. Phys. Chem. B **102**, 4441 (1998).

[14] T. Vallant, H. Brunner, U. Mayer, H. Hoffmann, T. Leitner, R. Resch, and G. Friedbacher, J. Phys. Chem. B **102**, 7190 (1998).

[15] A. G. Richter, M. K. Durbin, C.-J. Yu, and P. Dutta, Langmuir **14**, 5980 (1998).

[16] J. T. Woodward and D. K. Schwartz, J. Am. Chem. Soc. **118**, 7861 (1996).

[17] I. Doudevski, W. A. Hayes, and D. K. Schwartz, Phys. Rev. Lett. **81**, 4927 (1998).

[18] R. Resch, M. Grasserbauer, G. Friedbacher, T. Vallant, H. Brunner, U. Mayer, and H. Hoffmann, Appl. Surf. Sci. **140**, 168 (1999).

[19] T. Vallant, J. Kattner, H. Brunner, U. Mayer, and H. Hoffmann, Langmuir **15**, 5339 (1999).

[20] J. Als-Nielsen, D. Jacquemain, K. Kjaer, F. Leveiller, M. Lahav, and L. Leiserowitz, Phys. Rep. **246**, 251 (1994).

[21] M. Tolan and W. Press, Z. Kristallogr. **213**, 319 (1998).

[22] Z. Nagy, H. You, and R. M. Yonco, Rev. Sci. Instrum. **65**, 2199 (1994).

[23] P. Silberzan, L. Liger, D. Ausserri, and J. J. Benattar, Langmuir **7**, 1647 (1991).

[24] J. B. Brzoska, N. Shahidzadeh, and F. Rondelez, Nature (London) **360**, 719 (1992).

[25] C. P. Tripp and M. L. Hair, Langmuir **8**, 1120 (1992).

[26] A. N. Parikh, D. L. Allara, I. Ben Azuouz, and F. Rondelez, J. Phys. Chem. **98**, 7577 (1994).

[27] X. Zhao and R. Kopelman, J. Phys. Chem. **100**, 11 014 (1996).

[28] J. D. Le Grange, J. L. Markham, and C. R. Kurkjian, Langmuir **9**, 1749 (1993).

[29] D. A. Offord and J. H. Griffin, Langmuir **9**, 3015 (1993).

[30] R. Banga, J. Yarwood, and A. M. Morgan, Langmuir **11**, 618 (1995).

[31] C. P. Tripp and M. L. Hair, Langmuir **11**, 1215 (1995).

[32] A. N. Parikh, M. A. Schivley, E. Koo, K. Seshadri, D. Aurentz, K. Mueller, and D. L. Allara, J. Am. Chem. Soc. **119**, 3135 (1997).

[33] T. Nakagawa, K. Ogawa, and T. Kurumizawa, Langmuir **10**, 525 (1994).

[34] R. R. Rye, G. C. Nelson, and M. T. Dugger, Langmuir **13**, 2965 (1997).

[35] J. Gun and J. Sagiv, J. Colloid. Interface Sci. **112**, 457 (1986).

[36] R. Banga and J. Yarwood, Langmuir **11**, 4393 (1995).

[37] R. Banga, J. Yarwood, A. M. Morgan, B. Evans, and J. Kells, Thin Solid Films **284-285**, 261 (1996).

[38] D. A. Styrkas, J. L. Keddie, J. R. Lu, and T. J. Su, J. Appl. Phys. **85**, 868 (1999).

[39] H. Brunner, T. Vallant, U. Mayer, and H. Hoffmann, Langmuir **15**, 1899 (1999).

[40] A. Eberhardt, P. Fenter, and P. Eisenberger, Surf. Sci. **397**, L285 (1998).